

Multiband optical variability of the blazar OJ 287 during its outbursts in 2015 – 2016

Alok C. Gupta^{1,2*†}, Aditi Agarwal^{2‡}, Alka Mishra², H. Gaur¹, P. J. Wiita³, M. F. Gu¹, O. M. Kurtanidze^{4,5}, G. Damljanovic⁶, M. Uemura⁷, E. Semkov⁸, A. Strigachev⁸, R. Bachev⁸, O. Vince⁶, Z. Zhang¹, B. Villarroel⁹, P. Kushwaha¹⁰, A. Pandey², T. Abe⁷, R. Chanishvili⁴, R. A. Chigladze⁴, J. H. Fan¹¹, J. Hirochi⁷, R. Itoh¹², Y. Kanda⁷, M. Kawabata⁷, G. N. Kimeridze⁴, S. O. Kurtanidze⁴, G. Latev⁸, R. V. Muñoz Dimitrova⁸, T. Nakaoka⁷, M. G. Nikolashvili⁴, K. Shiki⁷, L. A. Sigua⁴, B. Spassov⁸

¹Shanghai Astronomical Observatory, Chinese Academy of Sciences, 80 Nandan Road, Shanghai 200030, China

²Aryabhata Research Institute of Observational Sciences (ARIES), Manora Peak, Nainital, 263 002, India

³Department of Physics, The College of New Jersey, P.O. Box 7718, Ewing, NJ 08628-0718, USA

⁴Abastumani Observatory, Mt. Kanobili, 0301 Abastumani, Georgia

⁵Engelhardt Astronomical Observatory, Kazan Federal University, 420 000 Tatarstan, Russia

⁶Astronomical Observatory, Volgina 7, 11060 Belgrade, Serbia

⁷Hiroshima Astrophysical Science Center, Hiroshima University, Kagamiyama 1-3-1, Higashi-Hiroshima 739-8526, Japan

⁸Institute of Astronomy and National Astronomical Observatory, Bulgarian Academy of Sciences, 72 Tsarigradsko Shosse Blvd., 1784 Sofia, Bulgaria

⁹Department of Physics and Astronomy, Uppsala Universitet, Box 516, 751 20, Uppsala, Sweden

¹⁰Department of Astronomy (IAG-USP), University of Sao Paulo, Sao Paulo 05508-900, Brazil

¹¹Center for Astrophysics, Guangzhou University, Guangzhou 510006, China

¹²Department of Physics, Tokyo Institute of Technology, 2-12-1 Ookayama, Meguro-ku, Tokyo 152-8551, Japan

Accepted ... Received ...; in original form ...

ABSTRACT

We present recent optical photometric observations of the blazar OJ 287 taken during September 2015 – May 2016. Our intense observations of the blazar started in November 2015 and continued until May 2016 and included detection of the large optical outburst in December 2016 that was predicted using the binary black hole model for OJ 287. For our observing campaign, we used a total of 9 ground based optical telescopes of which one is in Japan, one is in India, three are in Bulgaria, one is in Serbia, one is in Georgia, and two are in the USA. These observations were carried out in 102 nights with a total of ~ 1000 image frames in BVRI bands, though the majority were in the R band. We detected a second comparably strong flare in March 2016. In addition, we investigated multi-band flux variations, colour variations, and spectral changes in the blazar on diverse timescales as they are useful in understanding the emission mechanisms. We briefly discuss the possible physical mechanisms most likely responsible for the observed flux, colour and spectral variability.

Key words: galaxies: active – BL Lacertae objects: general – quasars: individual – BL Lacertae objects: individual: OJ 287

1 INTRODUCTION

Blazars are a subclass of radio loud active galactic nuclei and are further comprised of two classes, BL Lacertae objects, which have either very weak ($EW < 5\text{\AA}$) or no emission lines (Stocke et al.

1991; Marcha et al. 1996), and flat spectrum radio quasars with strong emission lines (e.g., Blandford & Rees 1978; Ghisellini et al. 1997). Blazars are primarily characterized by high brightness, high polarization in radio to optical bands, and highly variable, predominantly non-thermal emission across the entire electromagnetic (EM) spectrum. The emission is normally attributed to the relativistic jet aligned at a small angle with observer’s line of sight (LOS; e.g., Urry & Padovani 1995). The blazar emission over the entire

* Email: acgupta30@gmail.com

† CAS PIFI Visiting Scientist

‡ Email:aditi@aries.res.in

EM spectrum reveals the presence of a broad double peaked structures in their spectral energy distributions (SEDs). The presence of high polarization and its variation on timescales of the flux variation implies that the low energy peak (with usually between the IR and soft X-rays) of the blazar SED is result of synchrotron emission from relativistic non-thermal electrons in the jet. The high energy component, which peaks in gamma-rays somewhere between GeV and TeV energies probably originates from inverse Compton up-scattering of synchrotron or external photons off the relativistic electrons producing the synchrotron emission (Kirk, Rieger & Mastichiadis 1998; Gaur et al. 2010).

Blazar flux variations over the complete EM spectrum reveal diverse timescales with variability timescales extending from a few minutes to years and even decades. Flux variation from minutes to less than a day are commonly known as intraday variability (IDV) (Wagner & Witzel 1995) or intra-night variability or micro-variability (Goyal et al. 2012) while that from days to a few months is often called short term variability (STV) while flux variation over timescale of several months to years is usually called long term variability (LTV; Gupta et al. 2004). For most blazars the LTV and much of the STV can be explained through the shock-in-jet model (e.g. Marscher & Gear 1985; Hughes, Aller & Aller 1985). The most puzzling variability of blazars is that detected on IDV timescales, and understanding this may allow for probing the very inner region close the central black hole and might be helpful in measuring the mass of the central super massive black hole mass of blazars (Gupta et al. 2012). The first convincing optical flux variability on IDV timescale was reported by Miller et al. (1989) and since then it has been extensively studied by various groups around the globe (e.g. Carini et al. 1991, 1992; Carini & Miller 1992; Heidt & Wagner 1996; Sagar et al. 1999; Wu et al. 2005, 2007; Montagnani et al. 2006; Stalin et al. 2006; Gupta et al. 2008, 2016; Gaur et al. 2012a, 2012b, 2012c; Agarwal & Gupta 2015; Agarwal et al. 2015, 2016; and references therein). Optical variability of blazars on STV timescales are useful in exploring flux, colour and spectral variations and can also help to separate out any quasi-thermal (e.g. accretion disc emission) from the nonthermal emission component. We have done extensive work in this area (e.g. Gu et al. 2006; Fan et al. 1998, 2009; Gupta et al. 2008, 2016; Gaur et al. 2012b, 2012c; Agarwal et al. 2015, 2016 and references therein).

OJ 287 ($\alpha_{2000.0} = 08^{\text{h}} 54^{\text{m}} 48.87^{\text{s}}$, $\delta_{2000.0} = +20^{\circ} 06' 30.'' 64$) is a blazar at redshift $z = 0.306$ (Sitko & Junkkarinen 1985) that has relatively low frequency peaks for its SED. Its relative brightness means that it is one of the best observed blazars with more than a century of observations in the optical bands. Using this optical light curve data of OJ 287 starting in 1890, Sillanpää et al. (1988) noticed for the first time that there is double-peaked outburst feature which repeated with a period of ~ 12 yrs. To explain this unique quasi-periodic light curve feature Sillanpää et al. (1988) proposed a binary black hole system for this blazar and predicted next double-peaked outburst would occur in 1994 – 1995; this was indeed observed. In this case the second peak, occurring ~ 1.2 years after the detection of the first peak, was seen Sillanpää et al. (1996a, 1996b).

A double peaked outburst was also seen during the next recurrence in 2005 – 2007 with the outburst's first peak found at the end of 2005 and the second peak seen at the end of 2007 (Valtonen et al. 2009). These predicted recurrences are extremely strong evidence for OJ 287 housing a binary black hole system with a decaying orbital period of ~ 12 years. A puzzling issue in this model is the timing and strength of the second major peak of a outburst. In the first planned campaign in 1994 – 1995, the second peak was de-

tected ~ 1.2 years after the first peak (Sillanpää et al. 1996b) while it was observed ~ 2.0 years after the 1st peak during the 2005 – 2008 campaign (Valtonen et al. 2009).

The recurring outbursts of this source are not quite periodic and the quasi-periodic pattern of optical outbursts was explained by a model where a secondary black hole in a ~ 12 year orbit impacts the accretion disk of the primary black hole as it orbits the primary (Lehto & Valtonen 1996). The quasi-Keplerian nature of binary black hole orbits in general relativity mean that the times of the first impact flare and their associated radiation can be predicted (Memesheimer et al. 2004). The deviations from strict periodicity are understood in a model that contains a gravitational wave driven inspiraling spinning binary black hole system at its center (Valtonen et al. 2008; 2010). In this model, the impact outbursts are generated by expanding bubbles of hot gas that have been shocked and pulled out of the accretion disk (Lehto & Valtonen 1996; Pihajoki 2016). Hence, thermal radiation emanates from the vicinity of the impact site. Recently, the predicted first peak of the outburst was detected in December 2015 which is the brightest optical level in 30 years (Valtonen et al. 2016) and shows a clear signature of thermal emission. Valtonen et al. (2016) show that the data collected over the past three cycles give good measurements for the black hole masses, with the primary at $(1.83 \pm 0.01) \times 10^{10}$ and the secondary at $(1.5 \pm 0.1) \times 10^8$ solar masses. Remarkably, the spin of the primary can also be determined to high precision, at $a = 0.313 \pm 0.01$.

In the present work, we report detailed optical measurements of the late 2015 outburst OJ 287, including the detection of an a second outburst that is essentially as bright as the first one but occurred only ~ 3 months later. The paper is structured as follows: in Section 2, we discuss our new optical observations and data reduction, as well as public archival data used here. Section 3 gives information about the various techniques used in the work. In Section 4 we present results and give a discussion of them in Section 5. Our conclusions are summarized in Section 6.

2 OBSERVATIONS AND DATA REDUCTION

2.1 New Optical Observations and Data Reduction

Our optical photometric observing campaign of the blazar OJ 287 in B, V, R, and I passbands were carried out using telescopes in India, Bulgaria (3), Serbia, Georgia and Japan and correspond to telescopes *B* through *H* in the notes to Table 1. These telescopes are equipped with CCD detectors and broad band optical filters B, V, R, and I. Details of the CCDs mounted on telescopes B through F are reported in our earlier papers (Agarwal et al. 2015; Gupta et al. 2016). Information about telescopes G and H and their CCDs are given in Table 2. Telescope A corresponds to archival data from Steward Observatory.

We have performed multiband optical observations of the blazar OJ 287 (see Table 1) spanning the period between September 2015 and May 2016. These photometric observations include R band monitoring as continuously as we could manage so as to explore IDV. Quasi-simultaneous monitoring in BVRI filters were frequently made to study the day to day variations in the brightness and colour of the blazar. For the five telescopes *B* to *F* bias frames were taken at regular intervals during each night. Twilight sky flat-field frames were captured to get uniform light in the dawn and/or dusk of each observational night in all the filters. Observations were taken in the 1×1 , 2×2 and 3×3 binning mode on different telescopes to improve signal to noise (S/N) ratio as discussed earlier

Table 1. Observation log of optical photometric observations of the blazar OJ 287.

Date yyyy mm dd	Telescope	Data Points B, V, R, I	Date yyyy mm dd	Telescope	Data Points B, V, R, I	Date yyyy mm dd	Telescope	Data Points B, V, R, I
2015 09 20	A	00, 01, 01, 00	2016 01 12	A	00, 01, 01, 00	2016 03 12	A	00, 01, 01, 00
2015 10 13	A	00, 01, 01, 00	2016 01 12	F	01, 01, 01, 01	2016 03 13	A	00, 02, 02, 00
2015 10 14	A	00, 01, 01, 00	2016 01 13	A	00, 01, 01, 00	2016 03 14	A	00, 01, 01, 00
2015 10 15	A	00, 01, 01, 00	2016 01 14	A	00, 01, 01, 00	2016 03 15	A	00, 02, 02, 00
2015 10 29	G	00, 00, 04, 00	2016 01 14	H	00, 01, 01, 00	2016 03 16	A	00, 02, 02, 00
2015 11 10	A	00, 01, 01, 00	2016 01 15	A	00, 01, 01, 00	2016 03 16	G	00, 00, 04, 00
2015 11 11	A	00, 01, 01, 00	2016 01 16	A	00, 01, 01, 00	2016 03 17	A	00, 02, 02, 00
2015 11 12	A	00, 01, 01, 00	2016 01 18	A	00, 01, 01, 00	2016 03 30	G	00, 00, 08, 00
2015 11 12	F	01, 01, 01, 01	2016 01 19	A	00, 01, 01, 00	2016 03 31	G	00, 00, 09, 00
2015 11 13	A	00, 01, 01, 00	2016 01 20	G	00, 00, 04, 00	2016 04 01	G	00, 00, 04, 00
2015 11 13	G	00, 00, 03, 00	2016 01 30	H	00, 01, 01, 00	2016 04 03	G	00, 00, 04, 00
2015 11 14	A	00, 01, 01, 00	2016 02 03	G	00, 00, 05, 00	2016 04 05	E	02, 02, 02, 02
2015 11 18	A	00, 01, 01, 00	2016 02 04	G	00, 00, 04, 00	2016 04 06	E	02, 02, 02, 02
2015 12 04	F	01, 01, 01, 01	2016 02 05	G	00, 00, 04, 00	2016 04 08	B	01, 06, 06, 01
2015 12 05	F	01, 01, 01, 01	2016 02 06	G	00, 00, 06, 00	2016 04 10	B	01, 03, 03, 01
2015 12 06	F	01, 01, 01, 01	2016 02 06	F	01, 01, 01, 01	2016 04 11	G	00, 00, 07, 00
2015 12 07	G	00, 00, 17, 00	2016 02 07	H	00, 01, 01, 00	2016 04 11	B	01, 23, 23, 01
2015 12 08	G	00, 00, 04, 00	2016 02 07	F	01, 01, 01, 01	2016 04 12	B	01, 24, 24, 01
2015 12 08	F	01, 01, 01, 01	2016 02 09	A	00, 01, 01, 00	2016 04 13	B	01, 20, 20, 01
2015 12 09	A	00, 02, 02, 00	2016 02 10	A	00, 01, 01, 00	2016 04 13	A	00, 01, 01, 00
2015 12 09	G	00, 00, 08, 00	2016 02 11	A	00, 01, 01, 00	2016 04 14	A	00, 01, 01, 00
2015 12 10	A	00, 01, 01, 00	2016 02 11	H	00, 01, 01, 00	2016 04 14	H	00, 01, 01, 00
2015 12 10	G	00, 00, 14, 00	2016 02 12	A	00, 03, 03, 00	2016 04 16	G	00, 00, 06, 00
2015 12 11	G	00, 00, 09, 00	2016 02 13	A	00, 01, 01, 00	2016 04 18	H	00, 01, 01, 00
2015 12 12	G	00, 00, 11, 00	2016 02 14	A	00, 01, 01, 00	2016 04 26	E	03, 03, 03, 03
2015 12 12	F	01, 01, 01, 01	2016 02 15	A	00, 01, 01, 00	2016 04 27	E	09, 09, 09, 09
2015 12 12	C	01, 01, 04, 01	2016 02 15	G	00, 00, 18, 00	2016 04 27	D	01, 03, 03, 01
2015 12 12	E	02, 00, 02, 02	2016 02 16	A	00, 03, 03, 00	2016 04 29	B	01, 03, 03, 01
2015 12 13	G	00, 00, 07, 00	2016 02 17	H	00, 01, 01, 00	2016 05 01	G	00, 00, 11, 00
2015 12 13	F	01, 01, 01, 01	2016 02 17	G	00, 00, 06, 00	2016 05 03	A	00, 01, 01, 00
2015 12 13	C	01, 01, 04, 01	2016 02 25	H	00, 01, 01, 00	2016 05 03	H	00, 01, 01, 00
2015 12 13	E	02, 00, 02, 02	2016 02 29	H	00, 01, 01, 00	2016 05 04	A	00, 01, 01, 00
2015 12 14	A	00, 02, 02, 00	2016 02 29	G	00, 00, 04, 00	2016 05 05	A	00, 01, 01, 00
2015 12 14	F	01, 01, 01, 01	2016 03 01	G	00, 00, 04, 00	2016 05 06	A	00, 01, 01, 00
2015 12 14	C	01, 01, 06, 01	2016 03 01	E	02, 02, 02, 02	2016 05 06	H	00, 01, 00, 00
2015 12 14	E	02, 00, 02, 02	2016 03 02	G	00, 00, 06, 00	2016 05 08	A	00, 01, 01, 00
2015 12 15	F	01, 01, 01, 01	2016 03 02	E	02, 02, 02, 02	2016 05 09	A	00, 01, 01, 00
2015 12 15	D	01, 01, 06, 01	2016 03 03	G	00, 00, 04, 00	2016 05 10	A	00, 01, 01, 00
2015 12 16	A	00, 02, 02, 00	2016 03 04	G	00, 00, 02, 00	2016 05 11	A	00, 01, 01, 00
2015 12 17	D	01, 01, 04, 01	2016 03 05	G	00, 00, 05, 00	2016 05 11	H	00, 01, 01, 00
2015 12 18	G	00, 00, 35, 00	2016 03 06	G	00, 00, 02, 00	2016 05 13	D	01, 03, 03, 01
2015 12 19	G	00, 00, 33, 00	2016 03 06	F	01, 01, 01, 01	2016 05 14	D	01, 03, 03, 01
2015 12 21	G	00, 00, 06, 00	2016 03 07	H	00, 01, 00, 00	2016 05 17	H	00, 01, 01, 00
2015 12 26	G	00, 00, 08, 00	2016 03 09	A	00, 01, 01, 00	2016 05 20	H	00, 01, 01, 00
2015 12 26	H	00, 00, 01, 00	2016 03 10	A	00, 02, 02, 00	2016 05 31	C	02, 02, 02, 02
2016 01 06	H	00, 01, 01, 00	2016 03 11	A	00, 02, 02, 00			
2016 01 10	H	00, 01, 01, 00	2016 03 11	H	00, 01, 01, 00			

A: 2.3-m Bok Telescope and 1.54-m Kuiper Telescope at Steward Observatory, Arizona, USA

B: 1.04-m Sampuranand Telescope, ARIES, Nainital, India.

C: 2-m Ritchey-Chretien telescope at National Astronomical Observatory, Rozhen, Bulgaria.

D: 50/70-cm Schmidt telescope at National Astronomical Observatory, Rozhen, Bulgaria.

E: 60-cm Cassegrain telescope at Astronomical Observatory, Belogradchik, Bulgaria.

F: 60-cm Cassegrain telescope, Astronomical Station Vidojevica (ASV), Serbia

G: 70-cm meniscus telescope at Abastumani Observatory, Georgia

H: 1.5-m KANATA telescope at HigashiHiroshima Observatory, Japan

(Agarwal et al. 2015; Gupta et al. 2016). Image preprocessing involved the removal of detector effects through bias subtraction, flat fielding, edge trimming and cosmic ray removal which we did us-

ing standard procedures in IRAF¹. After the preprocessing we carry out the data reduction, for which standard photometry software, the

¹ IRAF is distributed by the National Optical Astronomy Observatories, which are operated by the Association of Universities for Research in

Table 2. Details of telescopes and instruments

	Abastumani, Georgia	KANATA, Japan
Telescope	70-cm Meniscus	1.5-m Ritchey-Chretien
CCD Model	Apogee Ap6E (KAF-1001)	Hamamatsu fully-depleted
Chip Size	1024 × 1024 pixels ²	2048 × 2048 pixels ²
Scale	2.4 arc sec pixel ⁻¹	0.29 arc sec pixel ⁻¹
Field	15 × 15 arcmin ²	10 × 10 arcmin ²
Gain	8 e ⁻¹ ADU ⁻¹	2.2 e ⁻¹ ADU ⁻¹
Read out noise	14 e ⁻¹ rms	5 e ⁻¹ rms
Typical Seeing	1 – 2 arcsec	1 – 2 arcsec

Dominion Astronomical Observatory Photometry (DAOPHOT II) (Stetson 1987; Stetson 1992), was used to obtain instrumental magnitude of the target and comparison stars. Since blazars fields are not crowded and we are interested only in the blazar and the comparison stars which are of comparable brightness, aperture photometry is sufficient to get their instrumental magnitudes. Other than our source, we also observed more than three local standard stars (e.g. Smith et al. 1985; Fiorucci & Tosti 1996; González-Pérez et al. 2001) in the same field of view to calibrate magnitude of the blazar and also to check for the presence of variability. Detailed descriptions of the data analysis are given in our earlier papers (e.g. Gaur et al. 2012c; Agarwal & Gupta 2015; Agarwal et al. 2015; Gupta et al. 2016; and references therein).

Observations of OJ 287 at the Abastumani Observatory were conducted from 2015 October 29 to 2016 May 1 at the 70 cm meniscus telescope (f/3) (telescope *G* hereafter). These measurements were made with an Apogee CCD camera Ap6E (1K × 1K, 24 μm² pixels) through a Cousins R filter. Reduction of the image frames was done using DAOPHOT II. An aperture radius of 5 arcsec was used for data analysis. The blazar data is calibrated using the local standard star number 4 in the field (Fiorucci & Tosti 1996).

We performed V and R band photometric observations of the blazar OJ 287 using the HONIR instrument installed on the 1.5 m Kanata telescope (telescope *H* hereafter) in the Higashi-Hiroshima Observatory, Japan (Akitaya et al. 2014). The data were reduced using standard procedures for CCD photometry. We performed aperture photometry using the APPHOT package in IRAF, and the blazar data is calibrated with the local standard star number 10 (Fiorucci & Tosti 1996).

2.2 Archival Optical Data

We also include recent optical photometric data taken from an archive of observations made at Steward Observatory, University of Arizona, USA². The observations are carried out using the 2.3m Bok and 1.54m Kupier telescopes. These are clubbed together as telescope *A* in the observation log presented in Table 1. These photometric observations of the blazar OJ 287 were made using the SPOL CCD Imaging/Spectropolarimeter mounted on those two telescopes. Details about the instrument, observation and data analysis are described in Smith et al. (2009).

Astronomy, Inc., under cooperative agreement with the National Science Foundation.

² <http://james.as.arizona.edu/psmith/Fermi/datause.html>

3 ANALYSIS TECHNIQUES

3.1 Variability detection criterion

To test for the presence blazar variability on intraday timescales we have used two standard statistics, the *F* and χ^2 tests (e.g., de Diego 2010). As pointed out by Romero et al. (2002), inappropriate selection of standard stars could lead to spurious variability detection. Thus we employed the two non-variable standard stars having magnitudes closest to OJ 287's magnitude. For calibration of the blazar magnitude we used the standard star having colour closer to the source.

3.1.1 *F*-Test

We quantify the blazar variability with the commonly used F-test (de Diego 2010) which is defined as

$$F_1 = \frac{\text{Var}(BL - StarA)}{\text{Var}(BL - StarB)}, \quad F_2 = \frac{\text{Var}(BL - StarA)}{\text{Var}(StarA - StarB)}. \quad (1)$$

Here (BL – Star A), (BL – Star B), and (Star A – Star B) are the differential instrumental magnitudes of blazar and Star A, blazar and Star B, and Star A and Star B, respectively, while Var(BL – Star A), Var(BL – Star B), and Var(Star A – Star B) are the variances of differential instrumental magnitudes.

An average of F_1 and F_2 gives the F value which is then compared with the critical $F_{\nu_{bl}, \nu_*}^{(\alpha)}$ value where α gives the significance level set for the test while ν_{bl} and ν_* signifies the number of degrees of freedom and is calculated as (N – 1) with N being the number of measurements. We have carried out the F test for α values 0.999 and 0.99 percent which correspond to essentially 3 σ and 2.6 σ detections of IDV, respectively. The higher the α values, the more reliable is the result. When the F value is greater than the critical value, the null hypothesis (no variability) is discarded. We consider LCs to be variable if $F > F_c(0.99)$.

3.1.2 χ^2 -Test

To further quantify the variability of the blazar we also used a χ^2 -test. The χ^2 statistic is defined as (e.g., Agarwal & Gupta 2015).

$$\chi^2 = \sum_{i=1}^N \frac{(V_i - \bar{V})^2}{\sigma_i^2}, \quad (2)$$

where, \bar{V} is the mean magnitude, and the *i*th observation gives a magnitude V_i with a corresponding standard error σ_i which is due to photon noise from the source and sky, CCD read-out plus other non-systematic error sources. Exact calculation of these errors by the IRAF reduction package is impractical. Theoretical errors have been found to be larger than the real errors by a factor of 1.3 – 1.75 (e.g., Gopal-Krishna et al. 2003). Thus, the errors obtained after data analysis should be multiplied by this factor, which was 1.5, to get better estimates of the real photometric errors. The average of χ^2 values is then compared with the critical value $\chi_{\alpha, \nu}^2$ where α is again the significance level and $\nu = N - 1$ is the number of degrees of freedom. Values of $\chi^2 > \chi_{\alpha, \nu}^2$ imply the presence of variability. We list sources as V only if they satisfy both the F-test and the χ^2 -test for $\alpha = 0.99$.

3.2 Percentage amplitude variation

The percentage of magnitude and colour variations on intraday or longer time scales are calculated using the variability amplitude

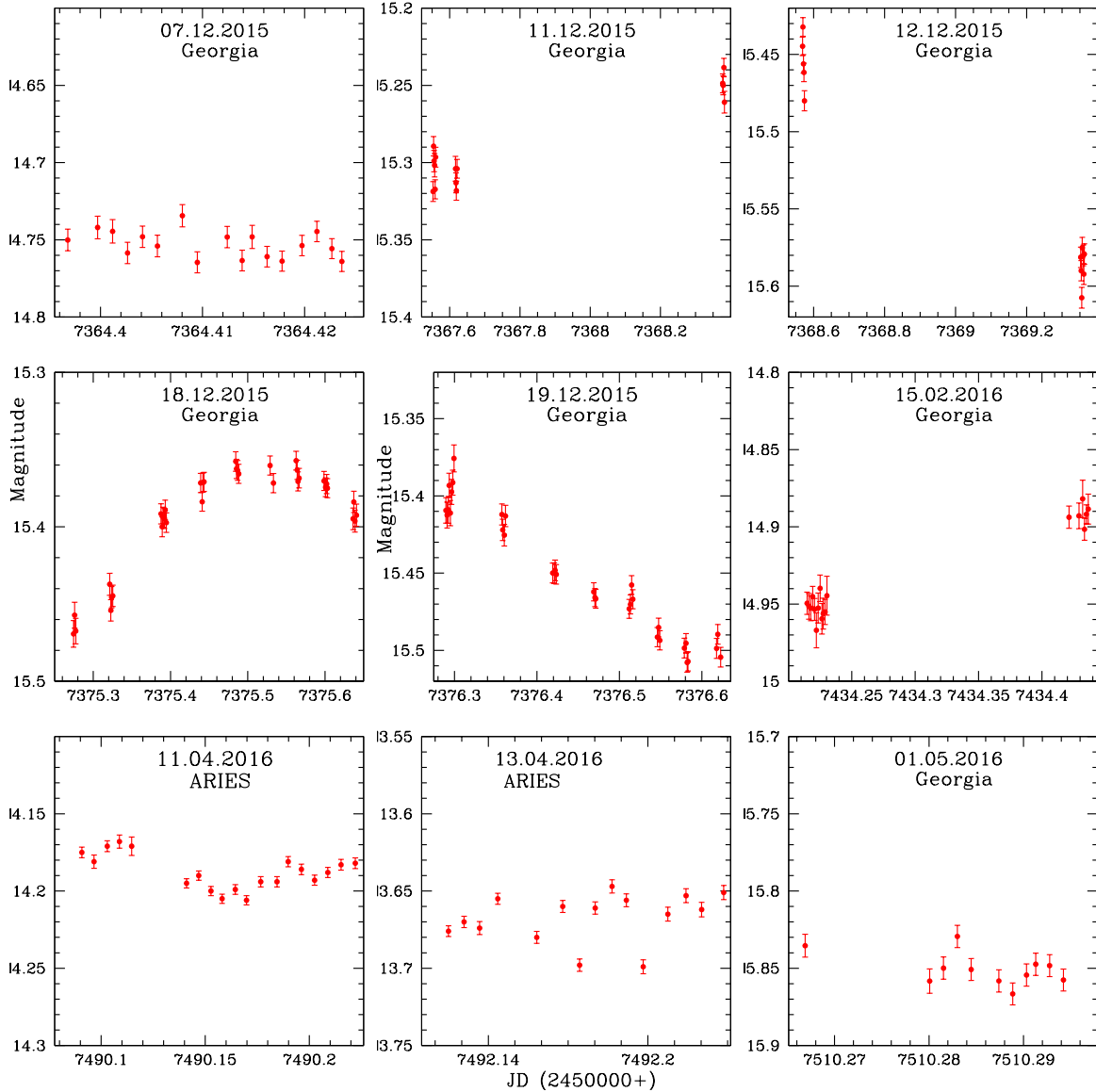


Figure 1. Intraday light curves for OJ 287 in R filter. The X axis is JD and the Y axis is the magnitude in each plot, where observation dates are indicated in each plot.

parameter A , introduced by Heidt & Wagner (1996), and defined as

$$A = 100 \times \sqrt{(A_{max} - A_{min})^2 - 2\sigma^2}(\%). \quad (3)$$

Here A_{max} and A_{min} are the maximum and minimum values in the calibrated magnitude and colour of LCs of the blazar, and σ is the average measurement error.

4 RESULTS

4.1 Intraday flux and colour variability

In searching for IDV, we used data from only those nights for which a minimum of 10 image frames of the blazar were taken in any specific optical passband. Using this criterion, sufficient observations of the blazar OJ 287 were carried out in the R passband on 10 nights and in the V passband on 3 nights between 2015 December

and 2016 May. The differential light curves of the blazar were extracted by following the data reduction procedure discussed above along with the differential instrumental magnitudes of the two best standard stars (e.g. Gupta et al. 2008) used for comparison (Star A – Star B). The calibrated derived LCs of the blazar are displayed in Fig. 1. V band LCs are not plotted due to their having worse data quality.

In order to investigate the presence or absence of variability during above nights we have followed the statistical analysis techniques described in section 3 with results summarized in Table 3. The blazar is marked as variable (V) if the variability conditions for both tests mentioned in Section 3 are satisfied; it is marked probably variable (PV) if conditions for one of the tests are followed, otherwise it is marked non-variable (NV). According to these conditions the target was found to be variable on five nights, possibly variable on one night and non-variable on four of the nights in the R passband. The blazar did not show any certain IDV in the V passband on any of the three nights it was observed, though it was prob-

Table 3. Results of IDV observations of OJ 287. Column 1 is the date of observation, column 2 indicates the band in which observations were taken, column 3 gives the number of data points in a particular band. In the next two columns i.e., 4 and 5, we have listed the results for the F-test and χ^2 -test, respectively, followed by variability status in column 6; finally the intra-day variability amplitude is given in column 7.

Date	Band	N	F-test	χ^2 test	Variable	A%
			$F_1, F_2, F, F_c(0.99), F_c(0.999)$	$\chi_1^2, \chi_2^2, \chi_{av}^2, \chi_{0.99}^2, \chi_{0.999}^2$		
07.12.2015	R	17	1.88, 2.41, 2.15, 3.37, 5.20	39.85, 69.42, 54.62, 32.00, 39.25	PV	–
11.12.2015	R	14	16.72, 10.34, 13.53, 3.91, 6.41	270.62, 218.99, 244.81, 27.69, 34.53	V	7.95
12.12.2015	R	12	176.08, 173.35, 174.72, 4.46, 7.76	2113.1, 2604.0, 2358.5, 24.72, 31.26	V	17.58
18.12.2015	R	35	43.74, 45.30, 44.52, 2.26, 2.98	1381.0, 1880.0, 1631.0, 56.06, 65.25	V	11.16
19.12.2015	R	33	54.38, 61.83, 58.10, 2.32, 3.09	1757.0, 2592.0, 2174.0, 53.49, 62.49	V	13.16
15.02.2016	R	12	0.81, 0.53, 0.67, 4.46, 7.76	12.59, 9.89, 11.24, 24.72, 31.26	NV	–
11.04.2016	V	22	1.57, 0.91, 1.24, 2.86, 4.13	22775, 89536, 56156, 38.93, 46.80	PV	–
	R	19	2.61, 4.07, 3.34, 3.13, 4.68	67.24, 209.37, 138.30, 34.80, 42.31	V	3.77
12.04.2016	V	24	0.04, 1.07, 0.56, 2.72, 3.85	4.89, 2.13, 3.51, 41.64, 49.73	NV	–
	R	24	2.00, 2.94, 2.47, 2.72, 3.85	131.08, 75.49, 103.29, 41.64, 49.73	NV	–
13.04.2016	V	18	1.22, 1.42, 1.32, 3.24, 4.92	0.03, 0.03, 0.85, 33.41, 40.79	NV	–
	R	17	1.00, 0.001, 0.50, 3.37, 5.20	1.66, 1.66, 0.85, 32.00, 39.25	NV	–
01.05.2016	R	11	11.18, 10.11, 10.65, 4.85, 8.75	102.20, 111.09, 106.65, 23.21, 29.59	V	7.67

V: Variable, PV: probable variable, NV: Non-Variable

ably variable on the one when the R-band was variable. The blazar was in a generally active state during our observation, as is most evident from the plots of 2015 December 11, 12, 18, 19 and 2016 April 11 and 1 May in Figure 1 when clear variability patterns were seen. We have not displayed 2016 April 12 light curve in Figure 1 due to poor quality data.

4.2 Short and long term flux and colour variation

We examined the short and long term flux and colour variability of the blazar. The overall LCs of OJ 287 are displayed in Figure 2 giving our multi-band optical observations during September 2015 – May 2016 for 103 observing nights. The BVRI passband LCs presented in the Figure 2 give clear evidence of large amplitude flux variability in all passbands on the timescale of days to weeks to months which gives clear evidence of flux variability on short and long timescales.

During our observation we found the blazar has varied from $\sim 14 - 16$ mag in B band, $\sim 13.4 - 15.4$ mag in V band, ~ 13 to 15.4 mag in R band, and ~ 12.5 to 14.4 mag in I band. Taking into account the noise, the variability amplitude on long term basis in B band was calculated as 199%, in V filter it was 222%, in R passband 231% while in I band it was calculated to be 192%. We also examined the (B-I), (V-R), (B-V), and (R-I) colour indices on short and long timescale to search for colour variability, and the results are plotted in Figure 3. While there were some modest apparent colour variations, we did not find any significant colour variability over a long term basis.

4.3 Colour-magnitude relationship

Since flux variations are often associated with changes in spectral shapes, we also studied the correlations between the colour indices and flux variations. Here we have considered whether variations in the (B-V), (V-R), (R-I) and (B-I) colour indices of the blazar change with respect to variations in its brightness in the V passband on short and long term bases. These colour and magnitude plots of OJ 287 are displayed in Fig. 4. We have calculated the best linear fit as shown by the straight lines in the Figure 4 for each colour index, Y , against magnitude, V : $Y = mV + c$. Fitted values for

Table 4. Color-magnitude dependencies and colour-magnitude correlation coefficients on short timescales.

Color Indices	m_1^a	c_1^a	r_1^a	p_1^a
(B-I)	0.029	1.565	0.191	0.331
(R-I)	-0.009	1.637	-0.103	0.588
(B-V)	-0.012	1.194	-0.105	0.594
(V-R)	0.016	-0.736	0.089	0.370

^a m_1 = slope and c_1 = intercept of CI against V;
 r_1 = Pearson coefficient; p_1 = null hypothesis probability

the slopes of the curves, m , and the constants, c , are listed in Table 4. We have also listed the linear Pearson correlation coefficients, r , and the corresponding null hypothesis probability values, p . Positive slope between the colour index and apparent magnitude of the blazar implies a positive correlation which further means that the source tends to be bluer when it is brighter (BWB) or redder when it is dimmer while a negative slope suggests an opposite correlation i.e. the source follows a redder when brighter (RWB) behaviour. Quite a few blazars have been found to show BWB behaviour (e.g., Raiteri et al. 2001; Villata et al. 2002; Papadakis et al. 2003; Agarwal & Gupta 2015). We find no significant negative or positive correlation between the V band magnitude and colour indices during these observations of OJ 287. Earlier studies (e.g., Raiteri et al. 2003; Wu et al. 2005; Stalin et al. 2006; Agarwal et al. 2016; and references therein) also found at the most weak or null evidence of spectral changes with the source brightness on short and long timescales. No spectral change with magnitude variations have been also reported by many authors in several other cases (e.g. Ghosh et al. 2000; Böttcher et al. 2007; Poon et al. 2009; and references therein).

4.4 Optical Spectral Energy Distribution

The SED is a simple but useful tool to diagnose the dominant emission components. Flux changes in blazars are often directly linked to the spectral changes, thereby making SED studies an important tool to learn details about the emission region, and can sometimes

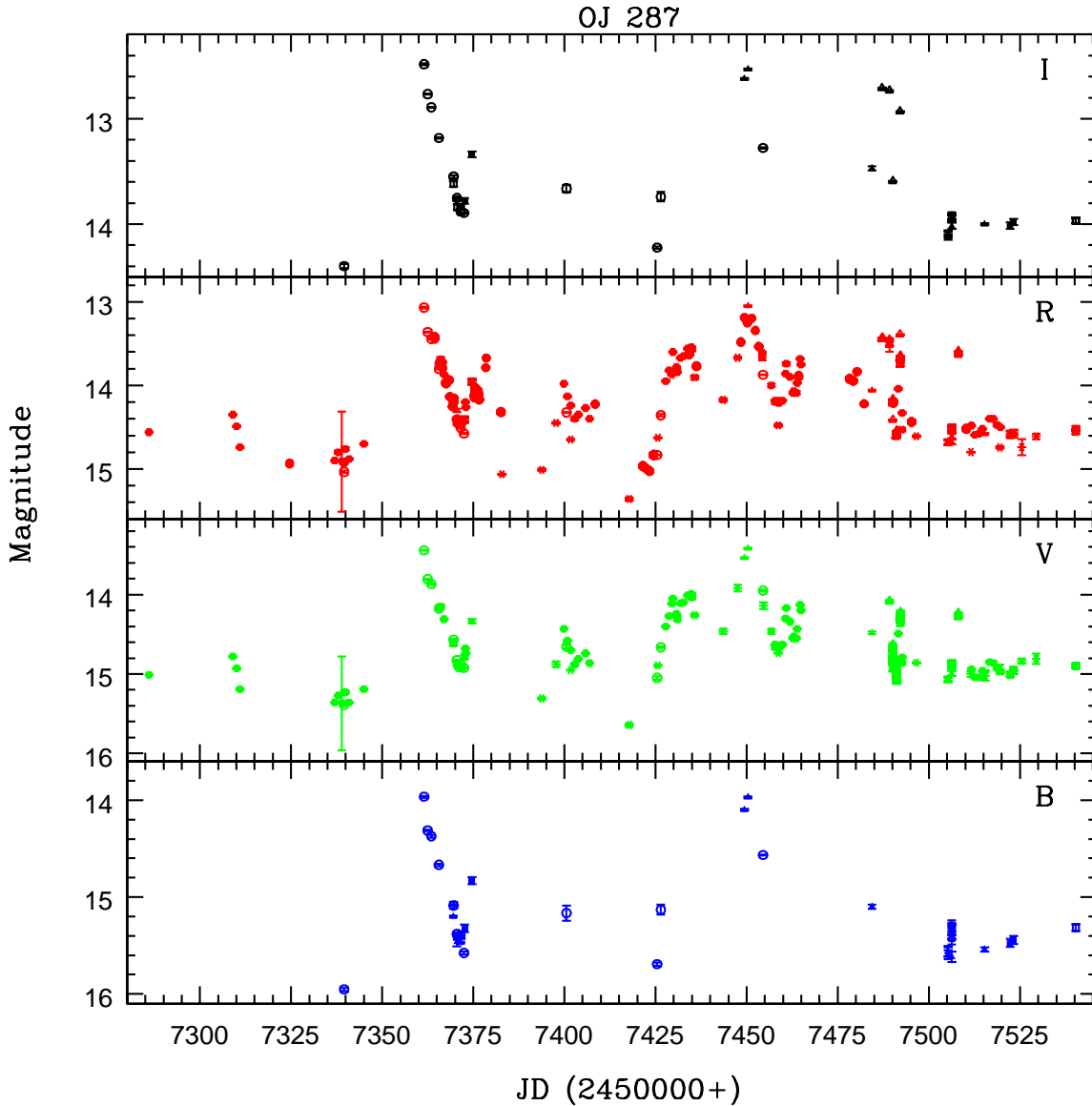


Figure 2. Optical variability light curve of OJ 287. Filled hexagon represent data from Arizona telescopes (A); open triangle for the data from 1.04m India telescope (B); open and filled square for the data from 2m (C) and 50/70 cm (D) telescopes Rozen, Bulgaria, respectively; filled triangle for the data from 60cm (E) telescope Belogradchik, Bulgaria; open circle for the data from 60cm (F) telescope, Serbia; filled circle for the data from 70cm (G) telescope, Georgia; and astrisk for the data from 1.5m (H) telescope, Kanata, Japan.

put tight constraints on the physical parameters such as the magnetic field, or energies of the relativistic particles in the Doppler boosted jet. To understand spectral variability in optical range, we used quasi-simultaneous B, V, R, and I data points at five different states of the source. The outburst state 1 is taken as that epoch when the source attained the brightest value in all four bands which lies near JD 2457361.5 (2015 Dec 5). We note that we do not have observations during the preceding two weeks so from our data the actual peak may have been even greater; however, the monitoring by Valtonen et al. (2016) had better coverage during the large flare and showed that it rose during that period and that the maximum brightness was reached on 2015 Dec 5. As is evident from the STV LC another very comparable outburst was observed around JD 2457450.4 (2016 March 2) which we call as outburst state 2 and which is covered well by our observations but not covered by

Valtonen et al. (2016). To quantify the spectral variability changes in the source during its faint state, we generated the SED around JD 2457339.6 (2015 Nov 13) when the source magnitude reached its maximum value. We also considered two stages in the post outburst state on JDs 2457369.6 (2015 Dec 13) and 2457372.4 (2015 Dec 15).

We have de-reddened the calibrated magnitudes of OJ 287 by subtracting Galactic absorption values of $A_B = 0.102$ mag, $A_V = 0.077$ mag, $A_R = 0.061$ mag, and $A_I = 0.042$ mag (Cardelli et al. 1989; Bessell et al. 1998). We took single data points in B, V, R, and I passbands, corresponding to the JDs for each of the above states and thus generated optical SEDs using our quasi-simultaneous B, V, R, and I observations of OJ 287. These SEDs are displayed in Figure 5. The faintest SED was observed for JD 2457339.6 while the brightest one was observed for JD 2457361.5.

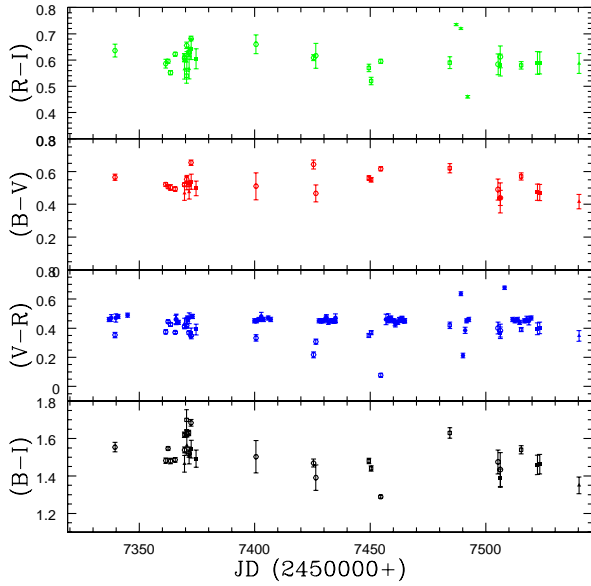


Figure 3. Optical colour variability light curves of OJ 287 covering the entire monitoring period.

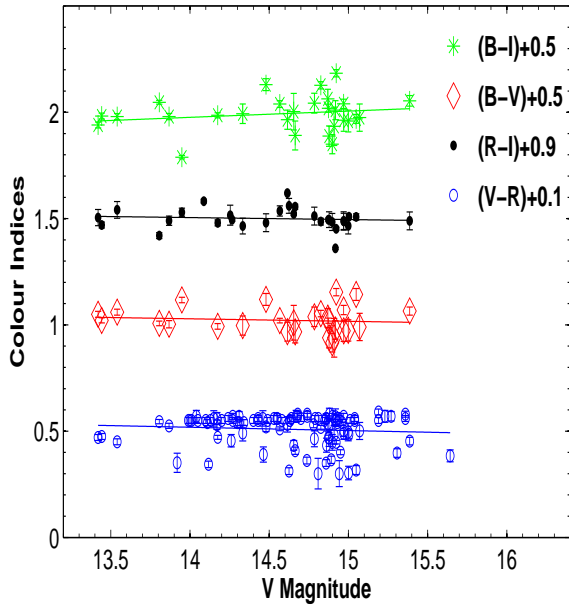


Figure 4. Optical colour-magnitude plots of OJ 287 during our monitoring.

Significant spectral changes are clearly evident from the figure as the source varied from its lowest brightness state to the highest one. The presence of a bump around the V-B bands is most visible in the SEDs corresponding to the post outburst state 2 and the Low state, as displayed in Fig. 5. The little blue bump might be attributed to the emission lines due to BLR region in the rest wavelength range $\sim 200 - 400$ nm (Raiteri et al. 2007), but in this case thermal emission from the accretion disc gas impacted by the secondary black hole is the most likely explanation (Valtonen et al. 2016). We also calculated the average spectral indices for above five epochs using (Wierzcholska et al. 2015),

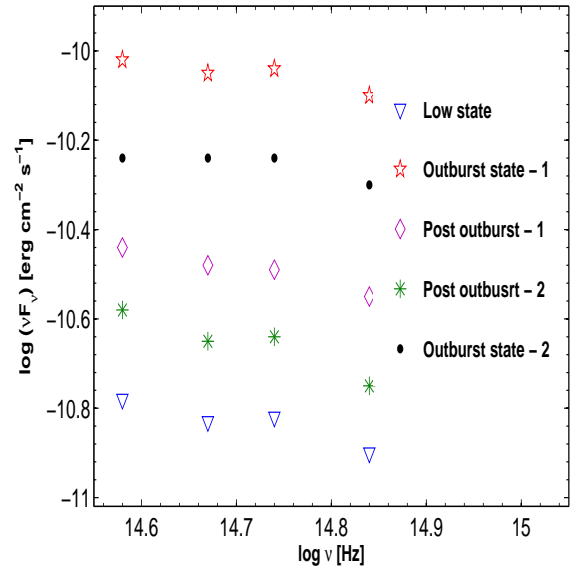


Figure 5. Optical SED of OJ 287 during different states. An offset of -0.2 for outburst state-2 is used to avoid its overlapping the SED of outburst state-1.

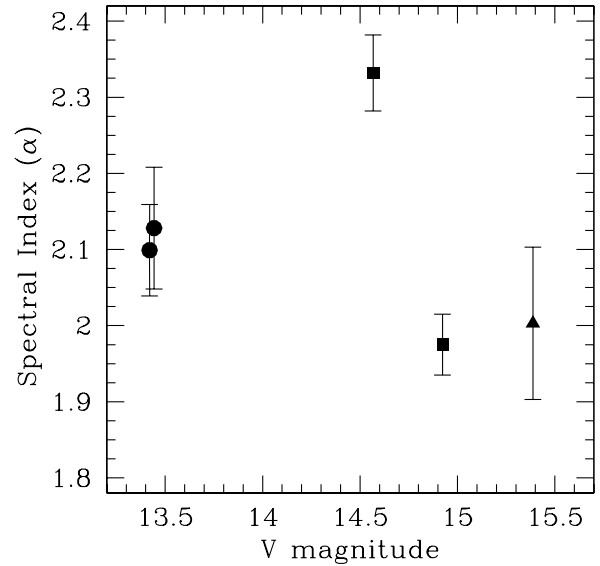


Figure 6. Variation of optical spectral index with V magnitude during outburst states (filled circles), post-outburst states (filled squares) and faint state (filled triangle) of OJ 287.

$$\langle \alpha_{VR} \rangle = \frac{0.4 \langle V - R \rangle}{\log(\nu_V / \nu_R)}, \quad (4)$$

where ν_V and ν_R are effective frequencies of the respective bands (Bessell, Castelli, & Plez 1998). The spectral index varied between 1.97 to 2.33 as is visible in Figure 6 where we have plotted spectral indices at various stages of the source vs the V band magnitude. The α_{VR} value for the low brightness state of the source was about 2.00 while for the outburst state 1 is ~ 2.13 . The higher values of spectral indices indicate synchrotron dominated emission

due to relativistic Doppler boosted jet emission (e.g. Kushwaha et al. 2013). Simultaneous multi-wavelength observations would be helpful in having detailed understanding of the spectral evolution of the target during its double outburst state.

4.5 Flaring and outbursts

Over the roughly nine months (September 2015 – May 2016) of our intense optical observing campaign of the blazar OJ 287, this source showed several unprecedented large amplitude flares seen best in the most densely observed R band data plotted in the second panel from the top in Figure 2. In our data there is a large gap during \sim JD 2457340 to JD 2457360 but that period was intensely monitored by Valtonen et al. (2016). The source went into an optical outburst at JD 2457342.5 \pm 2.5 (Valtonen et al. 2016) and reached the brightest value at $R \sim 13.05$ mag on JD 2457361.5 (i.e., in ~ 20 days) and then decayed to $R \sim 14.65$ mag at about JD 2457372 (i.e., in ~ 10 days). Then another flare started at about JD 2457372 at $R \sim 14.65$ which we observed as it reached $R \sim 13.6$ mag at about JD 2457372. A third significant flare started at about JD 2457423 when $R \sim 15$ mag and reached $R \sim 13.4$ in about 12 days or JD 2457435. The fourth large flare is one that could be considered a second outburst, as it reached $R \sim 13.05$ on about JD 2457450, when it had essentially the same brightness of the first outburst at maximum; however, in the binary black hole model, all of these flares would be considered to be part of the first outburst, with the second outburst expected to lag by at least a year. Another interesting feature in this overall outburst is that the largest flares seen during our monitoring (one and four) are separated by ~ 3 months.

5 DISCUSSION

Blazars, being dominated by jet emissions, display variability on a very wide range of timescales. The reason behind this blazar variability could be either intrinsic to the jet or due to changes in overall jet power. Shock-in-jet models (e.g., Marscher & Gear 1985; Spada et al. 2001; Graff et al. 2008; Joshi & Böttcher 2011) appear to explain the longer term variations quite well for most blazars. Changes in any of the physical parameters like velocity, electron density or magnetic field can trigger the emergence of a new shock which leads to high amplitude flares when propagating along the inhomogeneous medium of the relativistic jet. The moving shock causes acceleration of electrons to even TeV energies thus leading to radiation changes in all EM bands. Precession, helical structures or various other geometrical effects related to the Doppler boosted relativistic jet could lead to significant changes on STV timescales though they are probably more relevant for LTV ones (e.g. Camenzind & Krokenberger 1992; Pollack et al. 2016). Valtonen & Pihajoki (2013) have applied such a helical jet model to OJ 287. Some blazar variability can be also be extrinsic in nature. Such extrinsic mechanisms include refractive interstellar scintillations which, however, is only relevant for low frequency radio observations. Another extrinsic mechanism is gravitational microlensing which is applicable over the entire EM spectrum but is only relevant for lensed sources. Since we are reporting results based on multi-band optical observations of the blazar OJ 287 which is not a lensed system, extrinsic causes of variability are ruled out. Turbulence behind the shocks in a jet provide a good way of understanding much of the fastest variability seen from blazars (Marscher 2014; Calafut & Wiita 2015; Pollack et al. 2016). Blazar variability on IDV

timescale could be absent if there is no change in the speed or the direction of the propagating shock along the observer’s LOS. IDV and STV in quasars and perhaps in blazars during their low state can be attributed to instabilities in the accretion disc such as hot spots (e.g., Chakrabarti & Wiita, 1993; Mangalam & Wiita, 1993). Disturbances on or above the accretion disks are advected into the relativistic jet and thus, are Doppler amplified, which in turn might also provide seed fluctuations.

In the (so far) unique case of OJ 287 the strong flares occurring roughly every 12 years are almost certainly produced by large perturbations induced in the accretion disc around the primary super-massive black hole as the secondary black hole smashes through the disc (e.g. Lehto & Valtonen 1996; Valtonen et al. 2016). Because of the only quasi-Keplerian nature of the binary black hole orbits in general relativity and the impact of gravitational radiation on the orbits, the impact outbursts and their associated electromagnetic radiation will not be observed in a strictly periodic manner (Valtonen, Ciprini & Lehto 2012). In this model, thermal outbursts are generated by expanding bubbles of hot gas that have been shocked and pulled out of the accretion disc around the primary black hole. It was predicted that OJ 287 should show a major outburst in 2015 December (Valtonen et al. 2011). In our work, along with confirmation of this predicted major outburst during late 2015 also reported by Valtonen et al. (2016), we have found a comparably strong flare with a clear signature of a bump in the V and B bands after just 90 days. In the previous 2005–2007 cycle there was also a substantial event around 90 days after the primary outburst (Valtonen & Ciprini 2012), though it was not as relatively strong as we have found now. A possible explanation for this event is that it corresponds to a jet flare arising after this transfer time from the site of the impact to the base of the jet (Valtonen et al. 2006; Pihajoki et al. 2013). In the binary black hole model it expected that another comparable outburst will occur one to two years after the primary one, to parallel the gaps seen between the events during the previous two cycles in 1994–1995 and 2005–2007, so OJ 287 should continued to be monitored whenever possible.

Colour-magnitude (CM) correlations for blazars have been carried out by several authors on intraday as well as on short term bases (e.g. Papadakis et al. 2003, Sasada et al. 2010, Bonning et al. 2012, Gaur et al. 2012c, Agarwal & Gupta 2015). Such CM studies can elucidate the reason behind aspects of blazar variability and also help us to explore the emitting region. Significant BWB/RWB trends on diverse timescales with different slope values are well known in blazars (Gaur et al. 2012c, Agarwal et al. 2016) and are sensibly interpreted as arising from superpositions of red and blue emission components. For BWB situations the blue component can be ascribed to synchrotron emission from the Doppler boosted relativistic jet while the thermal emissions from the accretion disc could give the redder contribution. No clear BWB or RWB trends were found in these data. To be able to detect weaker CM relationships, we need to obtain very dense and highly precise simultaneous multi-band observations. These are needed because there are chances of non-negligible magnitude fluctuations occurring while changing from one filter to another during the quasi-simultaneous observations making it much more difficult to accurately measure colour changes.

6 CONCLUSIONS

We carried out multi-band optical photometric observations of the blazar OJ 287 during 103 observing nights between September

2015 – May 2016 using 10 ground based optical telescopes located all around the globe. We searched for flux variation on IDV, STV and LTV timescales, and for colour variations and any colour - magnitude relationship in the blazar time series data on STV and LTV timescales. Our main conclusions are following:

- We observed OJ 287 intensely enough to perform IDV studies in R and V passbands on 11 and 4 observing nights, respectively. We did not find significant IDV on any of the nights observed in the V band (though it was probably variable on one of them) while the blazar did show IDV in the R passband on 6 nights and possible IDV on 1 additional night.

- The blazar was in a highly active and variable state during our observing period, showing large amplitude flux variations on STV and LTV timescales. OJ 287 varied by $\sim 199\%$, 222% , 231% and 192% in the B, V, R and I passbands respectively.

- OJ 287 did not show any significant colour variations on STV and LTV timescales, nor did the colour–magnitude relationship indicate any significant spectral variations on those timescales.

- The blazar went through multiple flaring events during our observing run and there were four strong flares. The first flare occurred at the time predicted by the binary black hole model for OJ 287 (Valtonen & Ciprini 2012).

- OJ 287 again showed a major flare separated by ~ 90 days from the first one, and this last of the four flares we detected was exceptional in that it peaked at nearly the same magnitude as did the first.

ACKNOWLEDGMENTS

We thank the referee for constructive comments and suggestions. Data from the Steward Observatory spectropolarimetric monitoring project were used. This program is supported by Fermi Guest Investigator grants NNX08AW56G, NNX09AU10G, NNX12AO93G, and NNX15AU81G. ACG is partially supported by CAS President’s International Fellowship Initiative (PIFI) (grant no. 2016VMB073). HG is sponsored by the Chinese Academy of Sciences (CAS) Visiting Fellowship for Researchers from Developing Countries, CAS Presidents International Fellowship Initiative (grant no. 2014FFJB0005), supported by the NSFC Research Fund for International Young Scientists (grant no. 11450110398) and supported by a Special Financial Grant from the China Postdoctoral Science Foundation (grant no. 2016T90393). MFG is supported by the National Science Foundation of China (grants 11473054 and U1531245) and by the Science and Technology Commission of Shanghai Municipality (grant 14ZR1447100). AS, ES, RB work was partially supported by Scientific Research Fund of the Bulgarian Ministry of Education and Sciences under grant DO 02-137 (BIn-13/09). GD and OV gratefully acknowledge the observing grant support from the Institute of Astronomy and Rozhen National Astronomical Observatory, Bulgaria Academy of Sciences, via bilateral joint research project “Observations of ICRF radio-sources visible in optical domain”. This work is a part of the project nos. 176011 176004, and 176021 supported by the Ministry of Education, Science and Technological Development of the Republic of Serbia. The Abastumani Observatory team acknowledges financial support by the by Shota Rustaveli National Science Foundation under contract FR/577/6-320/13.

REFERENCES

- Agarwal A., Gupta A. C., 2015, MNRAS, 450, 541
 Agarwal A., et al., 2015, MNRAS, 451, 3882
 Agarwal A., et al., 2016, MNRAS, 455, 680
 Akitaya H., et al., 2014, SPIE, 9147, 40
 Bessell M. S., Castelli F., Plez B., 1998, A&A, 333, 231
 Blandford R. D., Rees M. J., 1978, PhysS, 17, 265
 Bonning E., et al., 2012, ApJ, 756, 13
 Böttcher M., et al., 2007, ApJ, 670, 968
 Calafut V., Wiita P. J., 2015, JApA, 36, 255
 Camenzind M., Krockenberger M., 1992, A&A, 255, 59
 Cardelli J. A., Clayton G. C., Mathis J. S., 1989, ApJ, 345, 245
 Carini M. T., Miller H. R., Noble J. C., Sadun A. C., 1991, AJ, 101, 1196
 Carini M. T., Miller H. R., 1992, ApJ, 385, 146
 Carini M. T., Miller H. R., Noble J. C., Goodrich B. D., 1992, AJ, 104, 15
 Chakrabarti S. K., Wiita P. J., 1993, ApJ, 411, 602
 de Diego J. A., 2010, AJ, 139, 1269
 Fan J. H., et al., 1998, A&AS, 133, 163
 Fan J. H., Zhang Y. W., Qian B. C., Tao J., Liu Y., Hua T. X., 2009, ApJS, 181, 466
 Fiorucci M., Tosti G., 1996, A&AS, 116, 403
 Gaur H., Gupta A. C., Lachowicz P., Wiita P. J., 2010, ApJ, 718, 279
 Gaur H., Gupta A. C., Wiita P. J., 2012a, AJ, 143, 23
 Gaur H., et al., 2012b, MNRAS, 420, 3147
 Gaur H., et al., 2012c, MNRAS, 425, 3002
 Ghisellini G., et al., 1997, A&A, 327, 61
 Ghosh K. K., Ramsey B. D., Sadun A. C., Soundararajaperumal S., 2000, ApJS, 127, 11
 González-Pérez J. N., Kidger M. R., Martín-Luis F., 2001, AJ, 122, 2055
 Gopal-Krishna, Stalin C. S., Sagar R., Wiita P. J., 2003, ApJ, 586, L25
 Goyal A., Gopal-Krishna, Wiita P. J., Anupama G. C., Sahu D. K., Sagar R., Joshi S., 2012, A&A, 544, A37
 Graff P. B., Georganopoulos M., Perlman E. S., Kazanas D., 2008, ApJ, 689, 68
 Gu M. F., Lee C.-U., Pak S., Yim H. S., Fletcher A. B., 2006, A&A, 450, 39
 Gupta A. C., Banerjee D. P. K., Ashok N. M., Joshi U. C., 2004, A&A, 422, 505
 Gupta A. C., Fan J. H., Bai J. M., Wagner S. J., 2008, AJ, 135, 1384
 Gupta A. C., et al., 2016, MNRAS, 458, 1127
 Gupta S. P., Pandey U. S., Singh K., Rani B., Pan J., Fan J. H., Gupta A. C., 2012, NewA, 17, 8
 Heidt J., Wagner S. J., 1996, A&A, 305, 42
 Hughes P. A., Aller H. D., Aller M. F. 1985, ApJ, 298, 301
 Joshi M., Böttcher M., 2011, ApJ, 727, 21
 Kirk J. G., Rieger F. M., Mastichiadis A., 1998, A&A, 333, 452
 Kushwaha P., Sahayanathan S., Singh K. P., 2013, MNRAS, 433, 2380
 Lehto H. J., Valtonen M. J., 1996, ApJ, 460, 207
 Mangalam A. V., Wiita P. J., 1993, ApJ, 406, 420
 Marcha M. J. M., Browne I. W. A., Impey C. D., Smith P. S., 1996, MNRAS, 281, 425
 Marscher A. P., Gear W. K., 1985, ApJ, 298, 114
 Marscher A. P., 2014, ApJ, 780, 87
 Memmesheimer R.-M., Gopakumar A., Schäfer G., 2004, PhRvD,

- 70, 104011
- Miller H. R., Carini M. T., Goodrich B. D., 1989, *Natur*, 337, 627
- Montagni F., Maselli A., Massaro E., Nesci R., Sclavi S., Maesano M., 2006, *A&A*, 451, 435
- Papadakis I. E., Boumis P., Samaritakis V., Papamastorakis J., 2003, *A&A*, 397, 565
- Pihajoki P., 2016, *MNRAS*, 457, 1145
- Pihajoki P., et al., 2013, *ApJ*, 764, 5
- Pollack M., Pauls D., Wiita P. J., 2016, *ApJ*, 820, 12
- Poon H., Fan J. H., Fu J. N., 2009, *ApJS*, 185, 511
- Raiteri C. M., et al., 2001, *A&A*, 377, 396
- Raiteri C. M., et al., 2003, *A&A*, 402, 151
- Raiteri C. M., et al., 2007, *A&A*, 473, 819
- Romero G. E., Cellone S. A., Combi J. A., Andruchow I., 2002, *A&A*, 390, 431
- Sagar R., Gopal-Krishna, Mohan V., Pandey A. K., Bhatt B. C., Wagner S. J., 1999, *A&AS*, 134, 453
- Sasada M., et al., 2010, *PASJ*, 62, 645
- Sillanpää A., Haarala S., Valtonen M. J., Sundelius B., Byrd G. G., 1988, *ApJ*, 325, 628
- Sillanpää A., et al., 1996a, *A&A*, 305, L17
- Sillanpää A., et al., 1996b, *A&A*, 315, L13
- Sitko M. L., Junkkarinen V. T., 1985, *PASP*, 97, 1158
- Smith P. S., Balonek T. J., Heckert P. A., Elston R., Schmidt G. D., 1985, *AJ*, 90, 1184
- Smith P. S., Montiel E., Rightley S., Turner J., Schmidt G. D., Jannuzi B. T., 2009, *arXiv*, arXiv:0912.3621
- Spada M., Ghisellini G., Lazzati D., Celotti A., 2001, *MNRAS*, 325, 1559
- Stalin C. S., Gopal-Krishna, Sagar R., Wiita P. J., Mohan V., Pandey A. K., 2006, *MNRAS*, 366, 1337
- Stetson P. B., 1987, *PASP*, 99, 191
- Stetson P. B., 1992, *ASPC*, 25, 297
- Stoeke J. T., Morris S. L., Gioia I. M., Maccacaro T., Schild R., Wolter A., Fleming T. A., Henry J. P., 1991, *ApJS*, 76, 813
- Urry C. M., Padovani P., 1995, *PASP*, 107, 803
- Valtonen M. J., et al., 2006, *ApJ*, 646, 36
- Valtonen M., Kidger M., Lehto H., Poyner G., 2008, *A&A*, 477, 407
- Valtonen M. J., et al., 2009, *ApJ*, 698, 781
- Valtonen M. J., et al., 2010, *ApJ*, 709, 725
- Valtonen M. J., Mikkola S., Lehto H. J., Gopakumar A., Hudec R., Polednikova J., 2011, *ApJ*, 742, 2
- Valtonen M., Ciprini S., 2012, *MmSAI*, 83, 219
- Valtonen M. J., Ciprini S., Lehto H. J., 2012, *MNRAS*, 427, 77
- Valtonen M. & Pihajoki P. 2013, *A&A*, 557, 28
- Valtonen M. J., et al., 2016, *ApJ*, 819, L37
- Villata M., et al., 2002, *A&A*, 390, 407
- Wagner S. J., Witzel A., 1995, *ARA&A*, 33, 163
- Wiercholska A., Ostrowski M., Stawarz Ł., Wagner S., Hauser M., 2015, *A&A*, 573, AA69
- Wu J., Peng B., Zhou X., Ma J., Jiang Z., Chen J., 2005, *AJ*, 129, 1818
- Wu J., Zhou X., Ma J., Wu Z., Jiang Z., Chen J., 2007, *AJ*, 133, 1599